

# Plumbing the Abyss: Black Ring Microstates

Iosif Bena<sup>(1)</sup>, Chih-Wei Wang<sup>(2)</sup> and Nicholas P. Warner<sup>(2)</sup>

<sup>(1)</sup> *Service de Physique Théorique,  
CEA Saclay, 91191 Gif sur Yvette, France*

<sup>(2)</sup> *Department of Physics and Astronomy, University of Southern California  
Los Angeles, CA 90089-0484, USA*

iosif.bena@cea.fr, chihweiw@usc.edu, warner@usc.edu

We construct the first smooth, horizonless “microstate geometries” that have the same charges, dipole charges and angular momenta as a BPS black ring whose horizon is macroscopic. These solutions have exactly the same geometry as black rings, except that the usual infinite throat is smoothly capped off at a very large depth. If the solutions preserve a  $U(1) \times U(1)$  isometry, then this depth is limited by flux quantization but if this symmetry is broken then the throat can be made arbitrarily deep by tuning classical, geometric moduli. Interpreting these “abysses” (smooth microstate geometries of arbitrary depth) from the point of view of the  $AdS$ -CFT correspondence suggests two remarkable alternatives: either stringy effects can eliminate very large regions of a smooth low-curvature supergravity solution, or the D1-D5-P CFT has quantum critical points. The existence of solutions whose depth depends on moduli also enables us to define “entropy elevators,” and these provide a new tool for studying the entropy of BPS and near-BPS black holes.

June, 2007

## 1. Introduction

While it is still uncertain whether it is a misnomer, the term “microstate geometries” has come to represent smooth, horizonless geometries that represent good string backgrounds, are asymptotic to  $\mathbb{R}^{n,1} \times \mathcal{C}$ , where  $\mathcal{C}$  is compact, and have the same charges as black holes or black rings. Given that such geometries exist at all (and apparently in large numbers) and that they provide semi-classical descriptions of microstates of black holes and black rings, it is important to investigate their physics. It is also very tempting to conjecture that these geometries could account for the entropy of black objects.

This conjecture leads to a host of interesting physical questions. Do “microstate geometries” represent extremely special, coherent states of the stringy black hole or can microstate geometries represent the “typical” microstates of a black hole and contribute significantly to its entropy? Are there enough classical microstate geometries to account for the black hole entropy? Is there a semi-classical quantization of these microstate geometries that leads to the correct black-hole entropy, at least to leading order? If so, can the typical microstate geometries be described in supergravity, or are they necessarily stringy? Many of these and related issues have been thoroughly analyzed for the two-charge system (see [1–12] for an incomplete list of relevant papers, and [13] for a review), and there is now very significant progress on the three-charge system (see [14–25] and [26] for a review), as well as for the four-dimensional [27–31] and non-BPS black-hole microstates [32,33].

One of the key steps in understanding three-charge microstate geometries was the realization that they are bubbling geometries, which come from the geometric transition of three-charge brane configurations [19,20,21]. Such a transition replaces the spatial  $\mathbb{R}^4$  that is used to construct the black-hole and black-ring solutions by a topologically non-trivial hyper-Kähler manifold. The singular sources that define the original black holes or black rings are replaced by smooth topological fluxes threading non-trivial cycles.

For reasons of computational simplicity, the metrics on the hyper-Kähler base were usually chosen to be Gibbons-Hawking (GH) metrics and microstate solutions constructed using these metrics have been analyzed extensively [19,20,21,25]. In particular, the asymptotic charges and angular momenta were computed and it was found that generic distributions of fluxes lead to microstate geometries whose charges correspond to maximally-

spinning classical black holes or black rings (of zero horizon area) [22]. We typically refer to such microstates geometries as “zero-entropy microstate geometries<sup>1</sup>.”

It is not known generically how to evade the restriction to zero-entropy microstates without introducing closed time-like curves (CTC’s). At present the only systematic way of doing this is to use mergers of zero-entropy microstates to obtain microstates of objects with non-zero entropy [34]. This technique was used in [23] to construct the first microstate solutions that have the same charges and angular momenta as a three-charge black hole of classically large horizon area, that is, a “true” black hole from the perspective of classical general relativity. In this paper we will also use both mergers of two zero-entropy black-ring microstates, as well as other methods, to obtain the first microstates of black rings with a classical horizon area. Note that because of the infinite non-uniqueness of BPS black rings [35,36,37], a solution with black ring charges and angular momenta is not necessarily a black ring microstate. A microstate has (by definition) *all* the macroscopic features of the object it describes, and for black ring this includes not only the charges and angular momenta, but also the dipole charges [38,39,35,36,37].

One of the interesting, and probably defining features of the microstates geometries of true black holes is that they are scaling solutions or “deep microstates.” That is, the “bubbles,” or non-trivial topological cycles scale into a vanishingly small region in the GH base metric (while preserving the relative sizes of the cycles). In the physical, space-time geometry this corresponds to the cycles descending deeply into a black-hole-like throat. Thus the bubbled black-hole geometries look like a regular black hole, except that their throat is capped off by regular geometry deep down the throat. In [23] it was shown that, at least for  $U(1) \times U(1)$  invariant geometries, the depth at which the capping-off occurs is set by the size of the smallest quantum of flux that one can place upon a single bubble. Moreover, it was shown that small, non-BPS fluctuations in the region of the cap have an energy (as measured from infinity) that matches the expected mass gap of typical states in the underlying D1-D5 conformal field theory (CFT). Thus these “deep microstates” should be interpreted as the holographic duals the long effective strings of the D1-D5 CFT.

Our purpose here is to study deep microstate geometries in more detail, focussing first on the mergers of bubbled supertube geometries that lead to microstate geometries

---

<sup>1</sup> One should, of course, remember that a microstate geometry is horizonless and smooth and necessarily has zero entropy. The phrase “zero-entropy microstate geometries” is meant to emphasize the fact that the corresponding classical black object with the same charges and angular momenta also has vanishing entropy.

of BPS black rings with a classically large horizon area (that is, “true” black rings). After reviewing some basic properties of bubbled geometries in Section 2, we begin in Section 3 by considering microstate geometries corresponding to a pair of supertubes and study the axially symmetric ( $U(1) \times U(1)$  invariant) mergers that lead to microstate geometries of “true” black rings. In Section 4 we find that this merger results in scaling, or deep, geometries where the non-trivial cycles descend deeply into the  $AdS$  throat of what looks like a classical black ring. The non-trivial topology, once again, smoothly caps off this throat at a depth that is set by the quantum of flux on an individual cycle. We thus obtain the analogs for black rings of the results that were found for black holes in [23].

The reader who is not keen on the technical details of the construction, and only interested in the physics of smooth microstate solutions of arbitrary depth can skip directly to Section 5, where we construct the first such example by considering a scaling solution that is no longer axi-symmetric. This solution has the surprising feature that the depth of the throat can be controlled by a modulus and can be made arbitrarily large by fine-tuning this modulus<sup>2</sup>. During this process the solution remains *completely smooth*. We will refer to such throats of arbitrary depth as *abysses*. The existence of abysses suggests that breaking the  $U(1) \times U(1)$  invariance allows the construction of smooth horizonless geometries whose holographic duals in the CFT exhibit mass gaps and spectra with energy gaps that are arbitrarily small. We discuss the interesting physics implied by the existence of these new solutions in Section 6. The properties of these solutions also suggest they can be used as “entropy elevators,” which could account for the entropy both of BPS and of non-BPS black holes. This idea is developed in Section 7.

**Note Added:** The day before this paper was submitted to the arXiv, the preprint [44] appeared, in which a horizonless three-charge scaling configuration with black ring charges is also constructed. From a four-dimensional perspective this configuration contains D6 and  $\overline{D6}$  branes, like the solutions we construct here, but also contains D0 branes. Hence, the five-dimensional lift of this solution, as well as of the solutions analyzed in [31], has a naked singularity corresponding to the D0 branes. Therefore, the solutions in [31,44] are useful for understanding and counting black hole microstates in the intermediate regime of parameters where the D4 branes affect the geometry and the D0’s are considered as probes. However, because of the naked singularity, their fate in the regime of parameters

---

<sup>2</sup> The solution we study is a five-dimensional, smooth solution that, from a four-dimensional perspective, corresponds to a “closed quiver” of D6 and anti-D6 branes [40–43].

where black holes and black rings have macroscopic horizons is unknown. In contrast, solutions with only D6 and  $\overline{\text{D6}}$  remain smooth in five dimensions, and hence give a valid description of microstates of black holes and black rings in the same region of the moduli space where the classical black holes and black rings also exist.

## 2. Bubbled Geometries

Before focussing on bubbled ring geometries, it is worthwhile reviewing some of the basics of bubbled geometries in general. For more details, see [20–23,26]. First recall that the four-dimensional base metric has Gibbons-Hawking (GH) form:

$$ds_4^2 = V^{-1} (d\psi + \vec{A} \cdot d\vec{y})^2 + V (d\vec{y} \cdot d\vec{y}), \quad (2.1)$$

where  $\vec{y} \in \mathbb{R}^3$  and

$$V = \sum_{j=1}^N \frac{q_j}{r_j}, \quad \vec{\nabla} \times \vec{A} = \vec{\nabla} V, \quad (2.2)$$

with  $r_j \equiv |\vec{y} - \vec{y}^{(j)}|$ . In order for the GH metric to be regular, one must take  $q_j \in \mathbb{Z}$  and for the metric to be asymptotic to that of flat  $\mathbb{R}^4$  one must also impose

$$q_0 \equiv \sum_{j=1}^N q_j = 1. \quad (2.3)$$

The fluxes through the non-trivial two-cycles in this geometry are determined by harmonic functions:

$$K^I \equiv \sum_{j=1}^N \frac{k_j^I}{r_j}, \quad (2.4)$$

and by the flux parameters,  $k_j^I$ , in particular. There is a gauge equivalence  $K^I \rightarrow K^I + c^I V$ , or  $k_j^I \rightarrow k_j^I + c^I q_j$  for any constant,  $c^I$ . It is therefore useful to define the gauge invariant flux parameters:

$$\tilde{k}_j^I \equiv k_j^I - q_j N k_0^I, \quad \text{with} \quad k_0^I \equiv \frac{1}{N} \sum_{j=1}^N k_j^I. \quad (2.5)$$

Following [20,21,23], the charges and angular momenta of a bubbled solution can be obtained from the positions,  $\vec{y}^{(j)}$ , of the GH points via:

$$Q_I = -2 C_{IJK} \sum_{j=1}^N q_j^{-1} \tilde{k}_j^J \tilde{k}_j^K, \quad (2.6)$$

$$J_R \equiv J_1 + J_2 = \frac{4}{3} C_{IJK} \sum_{j=1}^N q_j^{-2} \tilde{k}_j^I \tilde{k}_j^J \tilde{k}_j^K, \quad (2.7)$$

$$J_L \equiv J_1 - J_2 = 8 |\vec{D}|, \quad (2.8)$$

where  $N$  is the number of GH points and

$$\vec{D}_j \equiv \sum_I \tilde{k}_j^I \vec{y}^{(j)}, \quad \vec{D} \equiv \sum_{j=1}^N \vec{D}_j. \quad (2.9)$$

It is convenient to define:

$$P_{ij} \equiv \frac{1}{6} C_{IJK} \Pi_{ij}^{(I)} \Pi_{ij}^{(J)} \Pi_{ij}^{(K)} \quad (2.10)$$

and

$$\vec{J}_{Lij} \equiv -8 q_i q_j P_{ij} \hat{y}_{ij}, \quad \text{where} \quad \hat{y}_{ij} \equiv \frac{(\vec{y}^{(i)} - \vec{y}^{(j)})}{|\vec{y}^{(i)} - \vec{y}^{(j)}|}. \quad (2.11)$$

One then has [21,23]:

$$\vec{J}_L = \sum_{\substack{i,j=1 \\ j \neq i}}^N \vec{J}_{Lij}, \quad (2.12)$$

and if the GH points are all co-linear then we may take  $\hat{y}_{ij} = \pm 1$  and (2.12) reduces to a sum over  $\pm P_{ij}$ .

Finally, to eliminate CTC's near the GH points, this configuration must satisfy the bubble equations:

$$\sum_{\substack{j=1 \\ j \neq i}}^N q_i q_j \frac{P_{ij}}{r_{ij}} = - \sum_{I=1}^3 \tilde{k}_i^I, \quad (2.13)$$

where  $r_{ij} = |\vec{y}^{(i)} - \vec{y}^{(j)}|$

In this paper, we specifically wish to consider the situation where the bubbled geometry looks, at large scales, like a supertube or black ring. We therefore wish to take  $q_1 = +1$  and locate this GH point at  $\vec{y}^{(1)} = 0$  and will then assume that all the remaining GH points cluster a some distance,  $\rho$  from the origin. More specifically, we will typically assume that

$$r_{1j} \approx \rho, \quad r_{ij} \ll \rho, \quad i, j = 2, \dots, N. \quad (2.14)$$

In this limit, the first bubble equation yields the approximate ring radius:

$$\rho \approx - \left[ \sum_{I=1}^3 \tilde{k}_1^I \right]^{-1} \sum_{j=2}^N q_j P_{1j}. \quad (2.15)$$

### 3. The axi-symmetric merger of two bubbled supertubes

#### 3.1. The layout and physical parameters

We consider the simplest possible pair of bubbled rings in which each ring is bubbled by identical pairs of GH points of charges,  $-Q$  and  $+Q$ . Thus the configuration will have:

$$q_1 = +1, \quad q_2 = -Q, \quad q_3 = +Q, \quad q_4 = -Q, \quad q_5 = +Q, \quad (3.1)$$

and we will denote the various distances by

$$\rho \equiv r_{12}, \quad \sigma \equiv r_{34}, \quad \Delta_1 \equiv r_{23}, \quad \Delta_2 \equiv r_{45}. \quad (3.2)$$

This layout is depicted in Fig. 1. The  $\Delta_j$  will represent the bubbled ring widths, and in the classical limit,  $Q \rightarrow \infty$ , one has  $\Delta_j \rightarrow 0$ . In this limit,  $\rho$  and  $\rho + \sigma$  represent the classical supertube radii. The classical un-bubbled solution to which this bubbled solution corresponds was first constructed in [37,45].

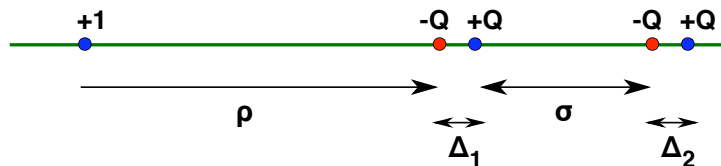


**Fig. 1:** The layout of GH points for two bubbled supertubes.

As usual we denote the flux parameters by

$$\Pi_{ij}^{(I)} = \left( \frac{k_j^I}{q_j} - \frac{k_i^I}{q_i} \right), \quad (3.3)$$

but there is a more natural, gauge invariant basis of flux parameters given by:

$$\begin{aligned} d_1^I &\equiv 2(k_2^I + k_3^I), & f_1^I &\equiv 2k_1^I + \left(1 + \frac{1}{Q}\right)k_2^I + \left(1 - \frac{1}{Q}\right)k_3^I, \\ d_2^I &\equiv 2(k_4^I + k_5^I), & f_2^I &\equiv 2k_1^I + \left(1 + \frac{1}{Q}\right)k_4^I + \left(1 - \frac{1}{Q}\right)k_5^I. \end{aligned} \quad (3.4)$$

In the classical supertube limit, where  $\Delta_j \rightarrow 0$ , the  $d^I$  reduce to the number,  $n^I$ , of M5 branes around the ring profile. In the GH metric these supertubes are point-like in the  $\mathbb{R}^3$  base and run around the  $U(1)$  fiber. The parameters,  $f_1^I$  and  $f_2^I$ , are a little more physically ambiguous but we have chosen them to be the gauge-invariant combinations of

flux parameters that are made out of the flux parameters associated to the two separate rings.

It is also easy to see how to define the  $d_a^I$  more generally in terms of the cohomology. Recall that the homology cycle,  $\Delta_{ij}$ , can be defined by the  $U(1)$  fiber running along any curve between  $q_i$  and  $q_j$ . The fluxes through  $\Delta_{23}$  and  $\Delta_{45}$  are simply  $\frac{Q}{2}d_1^I$  and  $\frac{Q}{2}d_2^I$  respectively. We also claim that  $\Delta_{23}$  and  $\Delta_{45}$  are homologous to the Gaussian surfaces that measure the M5-brane fluxes in the classical, supertube limit. To see this, first recall that for the GH points aligned along the  $z$ -axis we may take:

$$\vec{A} \cdot d\vec{y} = \sum_{j=1}^5 q_j \frac{(z - z_j)}{r_j} d\phi. \quad (3.5)$$

where  $\phi$  is the angle in the  $(x, y)$  plane. In particular, if  $V = \frac{1}{r}$  and  $\theta$  denotes the polar angle away from the  $z$ -axis then the GH metric reduces to that of  $\mathbb{R}^4 = \mathbb{R}^2 \times \mathbb{R}^2$ :

$$ds_4^2 = (du^2 + u^2 d\theta_1^2) + (dv^2 + v^2 d\theta_2^2), \quad (3.6)$$

via the coordinate transformation:

$$\begin{aligned} u &= \frac{1}{4} r^2 \cos \frac{\theta}{2}, & \theta_1 &= \frac{1}{2} (\psi + \phi), \\ v &= \frac{1}{4} r^2 \sin \frac{\theta}{2}, & \theta_2 &= \frac{1}{2} (\psi - \phi). \end{aligned} \quad (3.7)$$

Now observe that if one moves along the  $z$ -axis then the  $U(1)$  fiber direction,  $(d\psi + A)$ , is equal to  $2 d\theta_1 = d\psi + d\phi$  in the “long intervals” from  $q_1$  to  $q_2$ , from  $q_3$  to  $q_4$  and from  $q_5$  to infinity. In the supertube limit, the  $U(1)$  fiber, and hence the supertube, lies in the  $(u, \theta_1)$  plane. The Gaussian surfaces used to define M5-brane charge can be chosen to so that  $\theta_1$  is fixed and  $\theta_2$  is varying. This means they cannot involve  $\Delta_{12}$  and  $\Delta_{34}$ , which necessarily involve the fiber direction with co-tangent,  $(d\psi + A) \sim d\theta_1$ , and so the M5-brane Gaussian surfaces can only be related to  $\Delta_{23}$  and  $\Delta_{45}$ .

The charges and angular momenta of individual black rings are given by:

$$Q_I^{(a)} = C_{IJK} d_a^J f_a^K, \quad (3.8)$$

$$j_R^{(a)} \equiv \frac{1}{2} C_{IJK} (f_a^I f_a^J d_a^K + f_a^I d_a^J d_a^K) - \frac{1}{24} (1 - Q^{-2}) C_{IJK} d_a^I d_a^J d_a^K, \quad (3.9)$$

$$j_L^{(a)} \equiv \frac{1}{2} C_{IJK} (d_a^I f_a^J f_a^K - f_a^I d_a^J d_a^K) + \left( \frac{3Q^2 - 4Q + 1}{24Q^2} \right) C_{IJK} d_a^I d_a^J d_a^K, \quad (3.10)$$

for  $a = 1, 2$ .



For the configuration described above and depicted in Fig. 1 we have:

$$Q_I = Q_I^{(1)} + Q_I^{(2)} + C_{IJK} d_1^J d_2^K, \quad (3.11)$$

$$J_R = j_R^{(1)} + j_R^{(2)} + d_1^I Q_I^{(2)} + d_2^I Q_I^{(1)} + \frac{1}{2} C_{IJK} d_1^I d_2^J (d_1^K + d_2^K), \quad (3.12)$$

$$J_L = j_L^{(1)} + j_L^{(2)} + d_1^I Q_I^{(2)} - d_2^I Q_I^{(1)} + \frac{1}{2} C_{IJK} d_1^I d_2^J (d_1^K - d_2^K), \quad (3.13)$$

It is useful to introduce the flux vectors

$$Y^I \equiv (f_2^I - f_1^I - \frac{1}{2} (d_2^I - d_1^I)), \quad (3.14)$$

and the combination of fluxes:

$$\hat{P} \equiv (P_{24} - P_{25} - P_{34} + P_{35}) = \frac{1}{8Q^2} C_{IJK} d_1^I d_2^J Y^K. \quad (3.15)$$

Note that  $\hat{P}$  measures the total flux running between the pairs of points that define the two rings. The interaction part of the left-handed angular momentum can now be written:

$$\begin{aligned} J_L^{int} &\equiv d_1^I Q_I^{(2)} - d_2^I Q_I^{(1)} + \frac{1}{2} C_{IJK} d_1^I d_2^J (d_1^K - d_2^K) \\ &= 8Q^2 \hat{P} = C_{IJK} d_1^I d_2^J Y^K. \end{aligned} \quad (3.16)$$

From a four-dimensional perspective, the angular momentum  $J_L^{int}$  corresponds to the Poynting vector coming from the interaction of the electric fields of one ring with the magnetic fields of the other. We will see in the next sub-section that this controls the merger of the two rings.

### 3.2. Classical limits and their entropy

For a single, classical black ring, the entropy is given by

$$S = \pi \sqrt{\mathcal{M}} \quad (3.17)$$

where

$$\begin{aligned} \mathcal{M} &= 2 d^1 d^2 Q_1 Q_2 + 2 d^1 d^3 Q_1 Q_3 + 2 d^2 d^3 Q_2 Q_3 - (d^1 Q_1)^2 - (d^2 Q_2)^2 - (d^3 Q_3)^2 \\ &\quad - d^1 d^2 d^3 [4 J_L + 2 (d^1 Q_1 + d^2 Q_2 + d^3 Q_3) - 3 d^1 d^2 d^3], \end{aligned} \quad (3.18)$$

where  $J_L > 0$ , the  $d^I$  are the numbers of M5 branes and the  $Q_I$  are the electric charges measured from infinity. One also has the following relation between the angular momentum,  $J_L$ , and the classical embedding radius,  $R$ , measured in  $\mathbb{R}^2$ :

$$J_L = (d^1 + d^2 + d^3) R^2. \quad (3.19)$$

If one substitutes the expressions, (2.6) and (3.10), for the charges and for the angular momentum of a single, bubbled ring into (3.18), one obtains a simple expression:

$$\mathcal{M} = \left( \frac{4Q-1}{Q^2} \right) (d^1 d^2 d^3)^2. \quad (3.20)$$

Observe that this vanishes as  $Q \rightarrow \infty$ . This is the “classical limit” where the bubbled ring collapses back to the standard, classical ring. Therefore, the classical object corresponding to this simple, bubbled configuration has  $\mathcal{M} = 0$  and is thus a supertube.

For a bubbled ring, the relation, (3.19), emerges from the bubble equations as [20]:

$$J_L = 4(d^1 + d^2 + d^3) \rho. \quad (3.21)$$

where  $\rho$  is the ring radius measured in the GH base, and the change of variable (3.7) leads to  $\rho = \frac{1}{4}R^2$ .

If one merges two bubbled supertubes so as to obtain a single bubbled ring, one has an object with M5 brane charge given by  $d^I = d_1^I + d_2^I$  and with charges and angular momenta given by (3.11), (3.12) and (3.13). To obtain the entropy of the corresponding classical object, one substitutes these expressions into (3.18) and the result is:

$$\begin{aligned} \mathcal{M} = & -(\epsilon_{IJK} d_1^I d_2^J Y^K)^2 - 4 \left[ (d_1^1 + d_2^1)(d_1^2 d_1^3 d_2^1 + d_2^2 d_2^3 d_1^1) Y^2 Y^3 \right. \\ & + (d_1^2 + d_2^2)(d_1^1 d_1^3 d_2^2 + d_2^1 d_2^3 d_1^2) Y^1 Y^3 + (d_1^3 + d_2^3)(d_1^1 d_1^2 d_2^3 + d_2^1 d_2^2 d_1^3) Y^1 Y^2 \Big] \\ & - \frac{2}{3} (C_{IJK} (d_1^I + d_2^I)(d_1^J + d_2^J)(d_1^K + d_2^K)) (C_{ABC} d_1^A d_2^B Y^C) \\ & + \left( \frac{4Q-1}{36Q^2} \right) (C_{IJK} (d_1^I + d_2^I)(d_1^J + d_2^J)(d_2^K + d_2^K)) (C_{ABC} (d_1^A d_1^B d_1^C + d_2^A d_2^B d_2^C)). \end{aligned} \quad (3.22)$$

Note that if this is generically non-vanishing as  $Q \rightarrow \infty$ . However, if  $Y^I = 0$  then it does go to zero as  $Q \rightarrow \infty$ .

Putting it somewhat differently, if  $Y^I = 0$  then the merged ring has an effective  $d^I$  and  $f^I$  given by:

$$d^I = d_1^I + d_2^I, \quad f^I = f_1^I + \frac{1}{2} d_2^I = f_2^I + \frac{1}{2} d_1^I. \quad (3.23)$$

The fact that one adds the  $d_a^I$  follows from the considerations in Section 3.1 and the formula for  $f^I$  is obtained from (3.11) and (3.8), using  $Y^I = 0$ . Now observe that for large  $Q$ , one has

$$j_L^{(a)} \approx \frac{1}{2} C_{IJK} d_a^I (f_a^J - \frac{1}{2} d_a^J) (f_a^K - \frac{1}{2} d_a^K) = \frac{1}{2} C_{IJK} d_a^I (f^J - \frac{1}{2} d^J) (f^K - \frac{1}{2} d^K). \quad (3.24)$$

It then follows that when  $Y^I = 0$  the angular momentum,  $J_L$ , for the merged ring is given by:

$$\begin{aligned} J_L &= j_L^{(1)} + j_L^{(2)} + C_{IJK} d_1^I d_2^J Y^K = j_L^{(1)} + j_L^{(2)} \\ &\approx \frac{1}{2} C_{IJK} d^I (f^J - \frac{1}{2} d^J) (f^K - \frac{1}{2} d^K), \end{aligned} \quad (3.25)$$

which is the angular momentum,  $J_L$ , for a bubbled ring or supertube of charges  $d^I$  and  $Q_I$ . In other words the merged configuration still has a maximal value of  $J_L$  and the corresponding classical object still has vanishing horizon area. If  $Y^I \neq 0$  then the final angular momentum will generically be less than this maximal value<sup>3</sup>.

### 3.3. The bubble equations

For the configuration depicted in Fig. 1, there are four independent bubble equations (2.13). If one adds the equations for  $i = 2, 3$  and  $i = 4, 5$  then eliminates terms with denominators  $r_{23} = \Delta_1$  and  $r_{45} = \Delta_2$ , one obtains:

$$\begin{aligned} Q \left( \frac{P_{12}}{\rho} - \frac{P_{13}}{\rho + \Delta_1} \right) + Q^2 \Lambda &= -\frac{1}{2} \sum_{I=1}^3 d_1^I \\ Q \left( \frac{P_{14}}{\rho + \sigma + \Delta_1} - \frac{P_{15}}{\rho + \sigma + \Delta_1 + \Delta_2} \right) - Q^2 \Lambda &= -\frac{1}{2} \sum_{I=1}^3 d_2^I. \end{aligned} \quad (3.26)$$

where

$$\Lambda \equiv \frac{P_{24}}{\sigma + \Delta_1} - \frac{P_{34}}{\sigma} - \frac{P_{25}}{\sigma + \Delta_1 + \Delta_2} + \frac{P_{35}}{\sigma + \Delta_2}. \quad (3.27)$$

For two bubbled rings with  $\Delta_j \ll \rho, \sigma$ , assuming that all other terms in the multipole expansion are sub-leading, these equations reduce to:

$$\begin{aligned} \frac{Q(P_{12} - P_{13})}{\rho} + \frac{Q^2 \hat{P}}{\sigma} &= -\frac{1}{2} \sum_{I=1}^3 d_1^I \\ \frac{Q(P_{14} - P_{15})}{\rho + \sigma} - \frac{Q^2 \hat{P}}{\sigma} &= -\frac{1}{2} \sum_{I=1}^3 d_2^I. \end{aligned} \quad (3.28)$$

---

<sup>3</sup> This is not obvious from (3.22) because one must also require the absence of CTC's in the solution. This comment is therefore based primarily on the essential physics of mergers as well as experience with a number of examples.

For two generic bubbled rings to merge one must have  $\sigma \rightarrow 0$  and so the merger condition is  $\hat{P} \rightarrow 0$ , but with  $\sigma^{-1}\hat{P}$  remaining finite. Note that this means that the interaction part of the left-handed angular momentum,  $J_L^{int}$ , must vanish. More generally, for a solution in which  $\Delta_j$  and  $\sigma$  get small simultaneously, one must have  $\hat{P} \rightarrow 0$ , but with  $\Lambda$  remaining finite. Either way, the location,  $\rho_0$ , of the merged object is given by:

$$\begin{aligned}\rho_0 &= -2Q \left[ \sum_{I=1}^3 (d_1^I + d_2^I) \right]^{-1} (P_{12} - P_{13} + P_{14} - P_{15}) \\ &= \frac{1}{4} \left[ \sum_{I=1}^3 (d_1^I + d_2^I) \right]^{-1} \left( j_L^{(1)} + j_L^{(2)} + \frac{1}{6Q} C_{IJK} (d_1^I d_1^J d_1^K + d_2^I d_2^J d_2^K) \right),\end{aligned}\tag{3.29}$$

which is equivalent to (3.21) for the combined object.

Conversely, if one has  $\hat{P} \rightarrow 0$  one can obtain the merger solution, and a second solution in which  $\sigma$  remains finite. One then has:

$$\begin{aligned}\rho &= -2Q \left[ \sum_{I=1}^3 d_1^I \right]^{-1} (P_{12} - P_{13}) = \frac{1}{4} \left[ \sum_{I=1}^3 d_1^I \right]^{-1} \left( j_L^{(1)} + \frac{1}{6Q} C_{IJK} d_1^I d_1^J d_1^K \right), \\ \rho + \sigma &= -2Q \left[ \sum_{I=1}^3 d_2^I \right]^{-1} (P_{14} - P_{15}) = \frac{1}{4} \left[ \sum_{I=1}^3 d_2^I \right]^{-1} \left( j_L^{(2)} + \frac{1}{6Q} C_{IJK} d_2^I d_2^J d_2^K \right).\end{aligned}\tag{3.30}$$

Note that these are essentially the radii given by (3.21) for each of the two rings separately. Indeed, the limit  $\hat{P} \rightarrow 0$  corresponds to the vanishing of the “interaction part” of  $J_L$ .

In the foregoing merger analysis we have assumed that  $\Delta_j \ll \rho, \sigma$  and we have dropped terms from the multipole expansions of the denominators in (3.26). This means that the fluxes through the rings,  $\Pi_{23}^{(I)}$  and  $\Pi_{45}^{(I)}$ , must be much less than the other fluxes, and so  $Q^{-1}d_a^I$  must be small compared to  $f_a^I$  and  $d_a^I$ . Thus we should consistently drop terms that are sub-leading in  $Q^{-1}d_a^I$ , like the last terms in (3.29) and (3.30). Such terms also appear as corrections coming from the multipole expansions [23].

#### 4. Scaling solutions

A scaling solution is most simply defined to be a bubble configuration where there is a subset,  $\mathcal{S}$ , of the GH points that are uniformly approaching one another as some control parameter or, perhaps a modulus, is adjusted to a critical value. That is, one has

$$r_{ij} \rightarrow \lambda r_{ij}, \quad i, j \in \mathcal{S},\tag{4.1}$$

with  $\lambda \rightarrow 0$ . Physically, if the total charge of the GH points in  $\mathcal{S}$  is non-zero, this means that these GH points are descending into an arbitrarily deep black-hole-like throat and that the red-shifts of excitations localized around these points are going to infinity. Such black-hole microstates are called “Deep Microstates” and were discovered in [23] via the study of mergers of black holes and black rings [34]. In particular, scaling solutions were shown to be associated to microstates of black holes of non-zero horizon area and it was also argued (using the dual CFT) that these deep microstates belong to the same sector as the *typical* microstates of the black hole.

Here we examine the corresponding story when the total GH charge in  $\mathcal{S}$  is zero. One then expects to obtain scaling solutions corresponding to deep microstates of black rings with non-zero horizon area. This is, indeed what we find.

So far, the study of scaling solutions has largely focussed on  $U(1) \times U(1)$  invariant configurations. This is largely because such solutions are intrinsically simpler and, for fixed fluxes, there are finitely many, discrete solutions that are  $U(1) \times U(1)$  invariant. Moreover, in scaling solutions with such a symmetry, the depth of the throat is controlled by the choice of the quantized fluxes on bubbles [23], like  $\widehat{P}$  in Section 3. Thus the size of the flux quanta provides a cut-off for the maximum depth of the throat. However, one can easily break the  $U(1) \times U(1)$  symmetry to  $U(1)$  by letting the GH points move to arbitrary points,  $\vec{r}_i$ , in  $\mathbb{R}^3$  and then a subset of the angles between the vectors,  $\vec{r}_{ij} = \vec{r}_j - \vec{r}_i$ , become continuous moduli of the solutions. If the initial fluxes lie in the right domain then one can find scaling solutions at special points, or on special surfaces of the moduli space. Thus, we can make the black-hole, or black-ring throat arbitrarily deep by tuning the moduli. In practice, we find (numerically) that this tuning has to be extremely sharp and that the throat depth varies by many orders of magnitude for tiny (micro-radian) variations of the angles.

#### 4.1. Axi-symmetric scaling solutions

Since the  $U(1) \times U(1)$  invariant solutions are discrete for given fluxes, we can achieve an axi-symmetric scaling solution only by delicate adjustment of the fluxes. In particular, the easiest way to find such a scaling solution is via the merger of two bubbled supertubes as described in Section 3. Specifically, we need  $J_L^{int} \rightarrow 0$ , which means that the fluxes need to be adjusted so that  $\widehat{P} \rightarrow 0$ . To get a deep microstate, the expression for the classical horizon area, (3.22), shows that we must do this in such a manner that  $Y^I$  remains finite

and so the merger condition, (3.16), implies that we must tune the  $f^I$  or the  $d_a^I$  so that  $Y^I$  is finite but orthogonal to  $C_{IJK}d_1^J d_2^K$ .

It is relatively easy to see that there are scaling solutions that arise through mergers of bubbled supertubes. We consider, once again, the configuration in Fig. 1 where  $\Delta_j, \sigma \rightarrow 0$ . There are four independent bubble equations, (2.13), to satisfy. (Remember that the sum of the five bubble equations is trivial.) The first equation is precisely the same as the sum of the two equations in (3.26) and it determines the position,  $\rho_0$ , of the merger, as in (3.29). For the scaled merging of bubbled supertubes we expect that  $\Delta_j \ll \sigma$  during the merger and so the three remaining, independent bubble equations have the form:

$$\begin{aligned} -\frac{P_{25}}{\sigma + \Delta_1 + \Delta_2} - \frac{P_{23}}{\Delta_1} + \frac{P_{24}}{\sigma + \Delta_1} &\approx \frac{(P_{24} - P_{25})}{\sigma} - \frac{P_{23}}{\Delta_1} = C_1, \\ \frac{P_{23}}{\Delta_1} + \frac{P_{35}}{\sigma + \Delta_2} - \frac{P_{34}}{\sigma} &\approx \frac{(P_{35} - P_{34})}{\sigma} + \frac{P_{23}}{\Delta_1} = C_2, \\ -\frac{P_{24}}{\sigma + \Delta_1} + \frac{P_{34}}{\sigma} - \frac{P_{45}}{\Delta_2} &\approx \frac{(P_{34} - P_{24})}{\sigma} - \frac{P_{45}}{\Delta_2} = C_3, \end{aligned} \quad (4.2)$$

where the  $C_j$  contain terms involving the fluxes,  $Q$  and  $\rho_0$ . The important point about (4.2) is that we have explicitly shown the terms that grow large as  $\Delta_j, \sigma \rightarrow 0$ . For the scaling solution we need:

$$\sigma = \lambda \sigma^{(0)}, \quad \Delta_a = \lambda \Delta_a^{(0)}, \quad \lambda \rightarrow 0. \quad (4.3)$$

This means that, to leading order as  $\lambda \rightarrow 0$ :

$$\frac{\sigma^{(0)}}{\Delta_1^{(0)}} \approx \frac{(P_{24} - P_{25})}{P_{23}} \approx \frac{(P_{34} - P_{35})}{P_{23}}, \quad \frac{\sigma^{(0)}}{\Delta_2^{(0)}} \approx \frac{(P_{34} - P_{24})}{P_{45}}. \quad (4.4)$$

In particular there is no conflict between the first and second equations in (4.2) because  $\hat{P} \rightarrow 0$ . The foregoing solution becomes more and more accurate for smaller values of  $\lambda$  and given this solution one can then easily find the solution for finite, larger values of  $\lambda$  using perturbation theory.

This is not necessarily the only scaling solution with the configuration shown in Fig. 1. Indeed, numerical solutions show that there is often another one in which the  $\Delta_j$  and  $\sigma$  are of approximately the same order. However in all the examples of this second solution that we have found, there are large regions of CTC's. On the other hand, the scaling solutions that we have found based upon mergers of bubbled supertubes appear to be free of CTC's. We will discuss this more in Section 4.2.

#### 4.2. Numerical results for axi-symmetric scaling solutions

In order to see the scaling solutions explicitly, and verify that there are no CTC's we constructed several numerical examples and we now discuss a representative case.

It is useful to define:

$$X_a^I \equiv f_a^I - \frac{1}{2} d_a^I. \quad (4.5)$$

We then take  $Q = 105$  and:

$$\begin{aligned} d_1^I &= (50, 60, 40), & X_1^I &= (110, 560, 50), \\ d_2^I &= (80, 50, 45), & X_2^I &= (x, 270, 280), \end{aligned} \quad (4.6)$$

where  $x$  is varied from about 64 up to its merger value of  $x \approx 90.3$ . The results are shown in Fig. 2. As is evident from the graph, there are three sets of solutions to the bubble equations. Branch (i) exists for all values of  $J_L^{int}$  and has all four GH points in a very close cluster that scales as  $J_L^{int} \rightarrow 0$ . This appears as a very steep line at the center of Fig. 2. Branches (ii) and (iii) only appear at a bifurcation point when one has  $|J_L^{int}| \lesssim 43, 500$  or  $x \gtrsim 71.7$ , and represent solutions in which the four GH points separate into two sets of very close pairs. On branch (ii) the two pairs move apart as  $J_L^{int} \rightarrow 0$  and the locations of the two bubbled rings is given by (3.30). Branch (iii) is the scaling merger solution at  $\rho_0$  given by (3.29) and is described by (4.3) and (4.4).

We have done extensive numerical searches for CTC's in all these solutions and we find that branch (i) is completely unphysical, with large regions of CTCs, but that branches (ii) and (iii) are physical and have no CTC's.

Finally, one can use (3.18) or (3.22) to compute the horizon area,  $\mathcal{M}$ , of a classical black ring with the same charges and angular momenta as the merged configuration. The absolute number does not immediately convey useful information. On the other hand, we can compare this to the “maximal horizon area,”  $\mathcal{M}_0$ , of a black ring with the same values of  $Q_I$  and  $d^I$ , but with  $J_L = 0$ . For the configuration in (4.6) we find:

$$\mathcal{R} \equiv \frac{\mathcal{M}}{\mathcal{M}_0} \approx 0.14, \quad (4.7)$$

Thus the result of this merger of two bubbled supertubes is a microstate of a black ring with a non-vanishing horizon area.

We have studied several other such mergers with different values of flux parameters and found a number of solutions that are free of CTC's and have even higher values of  $\mathcal{R}$ .

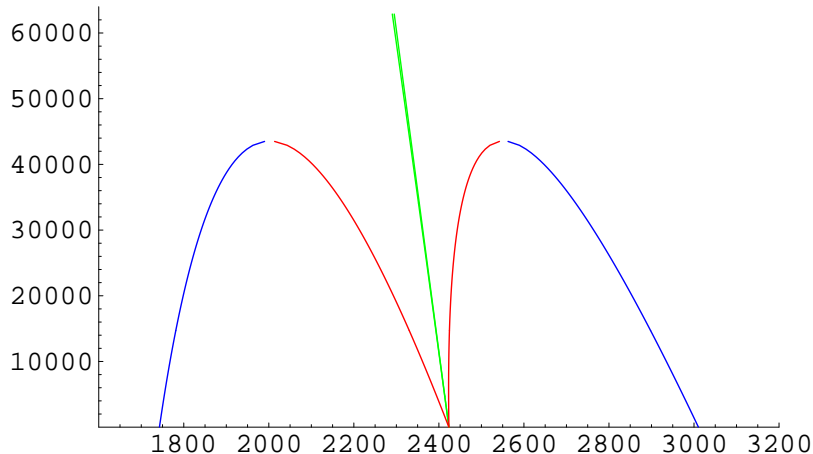


**Fig. 2:** Solutions of the bubble equations for the configuration shown in Fig. 1. The plot shows the ring positions,  $\rho$  and  $\sigma$ , along the horizontal axis with  $|J_L^{int}|$  plotted on the vertical axis. The separations,  $\Delta_j$ , are too small to resolve. There are three branches: (i) The single, nearly vertical line in the center (in green) for which all four GH points remain extremely close together; (ii) The two outermost curves (in blue) where the two rings become progressive more widely spaced as  $J_L^{int} \rightarrow 0$ ; (iii) The two curves (in red) that meet branch (ii) and show the scaling merger in which the two rings meet at  $J_L^{int} = 0$ .

Indeed, one can arrange a very high value of  $\mathcal{R}$  if one takes the outer ring to rotate in the opposite direction to the inner ring. One can achieve this in the foregoing example, (4.6), by taking, for example,

$$X_2^I = (-300, 270, 531.27), \quad (4.8)$$

while leaving all the other parameters unchanged. This configuration is very close to the merger point and has  $\mathcal{R} \approx 0.638$ . As one would expect, one generates more entropy by merging states whose angular momenta are opposed to one another.

## 5. Abysses and closed quivers.

Thus far we have primarily focussed on  $U(1) \times U(1)$  invariant scaling solutions. It is relatively easy to modify the analysis above to obtain scaling solutions in which the five GH points no longer lie on an axis. It is, however, even simpler to find scaling solutions based upon four GH points, and this is what we will focus on here.



Consider four charges laid out as in Fig. 3 with:

$$q_1 = +1, \quad q_2 = 2Q, \quad q_3 = -Q, \quad q_4 = -Q. \quad (5.1)$$

The general bubble equations take the form:

$$\begin{aligned} \frac{2Q P_{12}}{r_{12}} - \frac{Q P_{13}}{r_{13}} - \frac{Q P_{14}}{r_{14}} &= -\sum_{I=1}^3 \tilde{k}_1^I = C_1, \\ -\frac{2Q P_{12}}{r_{12}} - \frac{2Q^2 P_{23}}{r_{23}} - \frac{2Q^2 P_{24}}{r_{24}} &= -\sum_{I=1}^3 \tilde{k}_2^I = C_2, \\ \frac{Q P_{13}}{r_{13}} + \frac{2Q^2 P_{23}}{r_{23}} + \frac{Q^2 P_{34}}{r_{34}} &= -\sum_{I=1}^3 \tilde{k}_3^I = C_3, \\ \frac{Q P_{14}}{r_{14}} + \frac{2Q^2 P_{24}}{r_{24}} - \frac{Q^2 P_{34}}{r_{34}} &= -\sum_{I=1}^3 \tilde{k}_4^I = C_4, \end{aligned} \quad (5.2)$$

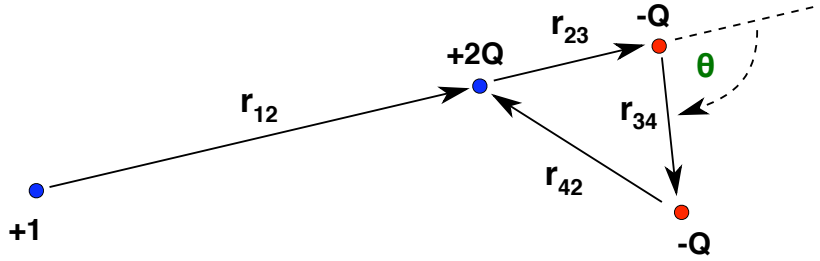


**Fig. 3:** The layout of GH points for a triangular scaling solution.

To obtain a scaling solution whose classical limit is a ring, the triangle defined by points 2, 3 and 4 should collapse so that:

$$r_{1j} \approx \rho, \quad r_{ij} \ll \rho, \quad i, j = 2, 3, 4. \quad (5.3)$$

Indeed, for a scaling solution in which  $r_{ij} \rightarrow 0$  for  $i, j = 2, 3, 4$ , the bubble equations (5.2) require that:

$$r_{ij} \rightarrow (-1)^{i+j+1} \lambda q_i q_j P_{ij}, \quad 2 \leq i < j \leq 4, \quad (5.4)$$

with  $\lambda \rightarrow 0$ . In other words, the fluxes define the lengths of the sides and hence the angles in the triangles. One then has:

$$\vec{J}_{Lij} = -8(-1)^{i+j+1} \lambda \vec{r}_{ij}, \quad 2 \leq i < j \leq 4, \quad (5.5)$$

where  $\vec{r}_{ij} \equiv (\vec{y}^{(i)} - \vec{y}^{(j)})$ . It follows that

$$\vec{J}_L^{int} = \sum_{i,j=2}^4 \vec{J}_{L\,ij} \rightarrow -16\lambda(\vec{r}_{23} + \vec{r}_{34} - \vec{r}_{24}) \equiv 0, \quad (5.6)$$

because these vectors define the sides of the triangle. The last bubble equation then yields:

$$\rho \approx 2Q \left[ \sum_{I=1}^3 d^I \right]^{-1} (P_{12} - 2P_{13} + P_{14}), \quad (5.7)$$

where

$$d^I \equiv 2(k_2^I + k_3^I + k_4^I). \quad (5.8)$$

Moreover, one also finds that the combination of fluxes in (5.7) is exactly the non-vanishing part of  $J_L$  and so one, once again, recovers (3.21).

Thus we find scaling solutions for generic values of fluxes: The only constraint is that the  $|q_i q_j P_{ij}|$  must satisfy the triangle inequalities. Now recall that only three of the equations in (5.2) are independent. One of them fixes  $\rho$  and the others fix the lengths of two sides of the triangle in terms of the length of the third side. Thus we may view the angle,  $\theta$ , in Fig. 3 as a modulus of the solution. The scaling solution then appears when the angle,  $\theta$ , is tuned so that the triangle has the shape determined by the fluxes as in (5.4). The new feature of this class of solutions is that we are no longer fine-tuning a quantized flux parameter in order to approach the scaling limit. For these triangular scaling solutions, one can pick the quantized fluxes and then the scaling solution appears as a *modulus* is tuned to a critical value.

Obviously, not all of these triangular scaling solutions will be free of CTC's and this will put further constraints on the flux parameters. However, we have found a number of numerical examples that exhibit scaling at the critical value of  $\theta$  and reveal no CTC's under careful numerical scrutiny of the solution. One such example has the following parameters:

$$\begin{aligned} q_i &= (1, 210, -105, -105), & k_i^1 &= (0, 525, 1200, 2210), \\ k_i^2 &= (0, -20000, 16000, 7887), & k_i^3 &= (0, 6400, 1613, 7900), \end{aligned} \quad (5.9)$$

where,  $i = 1, \dots, 4$ . Define  $\Gamma_{ij} = q_i q_j P_{ij}$  then we have:

$$\Gamma_{23} = 8.0446 \times 10^8, \quad \Gamma_{34} = 4.9063 \times 10^8, \quad \Gamma_{24} = -1.1046 \times 10^9. \quad (5.10)$$

Note that the magnitudes of these fluxes all satisfy the triangle inequalities

$$|\Gamma_{ij}| \leq |\Gamma_{ik}| + |\Gamma_{kj}|. \quad (5.11)$$

By solving the bubble equations numerically, we find the overall size of the ring blob depends on the shape of the triangle formed by the three charges. In Table 1 we show how the size of the triangle changes as we vary the angle,  $\theta$ .

The total dipole charges of this merger solution are given by:

$$d^I \equiv 2 \sum_{j=1}^3 k_j^I, \quad (5.12)$$

while the electric charges and angular momenta can be obtained from (2.6), (2.7) and (2.8). From these one can obtain the horizon area ratio,  $\mathcal{R}$ , in (4.7) for the corresponding classical black-ring solutions and here we find  $\mathcal{R} \approx 0.103$ . Thus this scaling solution represents a microstate of a true black ring.

| $\pi - \theta$ | $r_{12}$ | $r_{23}$                | $r_{34}$                | $r_{24}$                | $r_{34}/r_{23}$ | $r_{24}/r_{23}$ |
|----------------|----------|-------------------------|-------------------------|-------------------------|-----------------|-----------------|
| 0              | 580.889  | 28.601                  | 19.150                  | 47.751                  | .66954          | 1.6695          |
| .2             | 532.623  | 27.820                  | 18.577                  | 46.175                  | .66776          | 1.6598          |
| .4             | 537.742  | 25.439                  | 16.851                  | 41.482                  | .66238          | 1.6306          |
| .6             | 546.005  | 21.341                  | 13.943                  | 33.779                  | .65333          | 1.5828          |
| .8             | 557.025  | 15.323                  | 9.8136                  | 23.251                  | .64046          | 1.5174          |
| 1              | 570.302  | 7.0865                  | 4.4196                  | 10.178                  | .62366          | 1.4363          |
| 1.1            | 577.612  | 2.0172                  | 1.2381                  | 2.8049                  | .61375          | 1.3905          |
| 1.13           | 579.878  | .36089                  | .22035                  | .49664                  | .61058          | 1.3762          |
| 1.136          | 580.335  | .021823                 | .013311                 | .029969                 | .60993          | 1.3732          |
| 1.13635        | 580.361  | $1.963 \times 10^{-3}$  | $1.197 \times 10^{-3}$  | $2.695 \times 10^{-3}$  | .60990          | 1.3731          |
| 1.136383       | 580.364  | $9.008 \times 10^{-5}$  | $5.494 \times 10^{-5}$  | $1.237 \times 10^{-5}$  | .60989          | 1.3731          |
| 1.136384586    | 580.364  | $6.289 \times 10^{-8}$  | $3.836 \times 10^{-8}$  | $8.635 \times 10^{-8}$  | .60989          | 1.3731          |
| 1.1363845871   | 580.364  | $4.573 \times 10^{-10}$ | $2.789 \times 10^{-10}$ | $6.279 \times 10^{-10}$ | .60989          | 1.3731          |
| 1.136384587108 | 580.364  | $3.207 \times 10^{-12}$ | $1.956 \times 10^{-12}$ | $4.403 \times 10^{-12}$ | .60989          | 1.3731          |

**Table 1:** This table shows the distances,  $r_{ij}$ , between point  $i$  and point  $j$  in the triangle solution as a function of the modulus,  $\theta$ . (See Fig. 3.) The angle,  $\theta$ , is the angle between  $\vec{r}_{23}$  and  $\vec{r}_{34}$  and it is varied to produce the merger at  $\theta = \theta_c$  (given below), while all the other parameters are kept fixed. One should also note that the ratios of the distances at merger are precisely the ratios of the fluxes:  $|\Gamma_{34}/\Gamma_{23}| \approx 0.609893$  and  $|\Gamma_{24}/\Gamma_{23}| \approx 1.37308$ .

As the angle  $\theta$  is changed towards a critical angle, given by

$$\pi - \theta_c \approx 1.13638458710805705... \quad (5.13)$$

the distances inside the ring blob as measured on the base  $(r_{23}, r_{34}, r_{24})$  shrink as well, such that

$$r_{ij} \sim \theta - \theta_c \quad (5.14)$$

We have checked at great length that this solution is free of closed timelike curves and has a global time function. Some details of the investigation are presented in the Appendix.

As explained in [23,26], during the scaling (5.14) the physical distances between the points that form the cap remains the same, while the throat becomes longer and longer<sup>4</sup>. The structure of the cap remains self-similar, the curvature is bounded above by a cap-dependent value that is parametrically smaller than the Planck size. Hence, supergravity is a valid description of the scaling solution for any throat depth! Interestingly-enough, as  $\theta \rightarrow \theta_c$ , the length of the throat diverges, and the solution becomes an “abyss” that increasingly resembles the naive black hole solution.

From a four-dimensional perspective, the solutions we consider here correspond to multi-centered configurations of D6 and  $\overline{\text{D6}}$  branes. The fact that four-dimensional multi-center solutions can collapse has been known for quite a while [40–42] (see [43] for recent progress) and has been associated to the existence of “closed quivers” in the gauge theory describing these configurations. The discussion of fluxes and angular momenta presented above can also be obtained from the more general analysis of multi-black hole four-dimensional solutions, upon restricting to D6 –  $\overline{\text{D6}}$  configurations.

It is also possible to argue from a four-dimensional perspective that even if the points of the quiver appear to collapse, in fact the distance between these points remains fixed<sup>5</sup>. The four-dimensional metric is

$$ds_{4D}^2 = -\mathcal{Q}^{-1/2}(dt + \omega)^2 + \mathcal{Q}^{1/2}(ds_{\mathbb{R}^3}^2) \quad (5.15)$$

where

$$\mathcal{Q} \equiv Z_1 Z_2 Z_3 V - \mu^2 V^2 \geq 0. \quad (5.16)$$

---

<sup>4</sup> We have also checked this explicitly for the solution presented in Table 1.

<sup>5</sup> We thank Eric Gimon for pointing out this argument to us.

In a scaling solution where the distances between the centers in the flat  $\mathbb{R}^3$  metric scales like  $\Lambda$ , the value of the function  $\mathcal{Q}$  in the region of the centers scales like  $1/\Lambda^2$ , when the total charge of the scaling centers is that of a black hole of non-zero entropy. Hence, the physical distance between the scaling centers remains constant. This four-dimensional analysis also implies that only centers whose total charge corresponds to a black hole or a black ring of finite horizon area can form a deep (abyssal) microstate.

Of course, from a four-dimensional perspective all the GH centers are naked singularities, and one could object that the distances between these centers are ill-defined. However, the four-dimensional results are useful because they complement those obtained from the full five-dimensional solution: the physical distance between the centers remains fixed throughout the scaling, and the apparent collapse of the centers manifests itself as the appearance of a throat.

## 6. The physics of deep microstates and abysses

We have found the first examples of smooth microstate geometries that have the same charges, dipole moments and angular momenta as black rings with a macroscopically large horizon area. These solutions are identical to black-ring solutions, both in the asymptotic region, and in the near-horizon region, but instead of having the infinite throat of classical BPS black rings, they have a very deep throat that ends in a smooth cap. All the charges of the solution come from fluxes threading topologically non-trivial cycles at the bottom of the throat.

If we impose  $U(1) \times U(1)$  symmetry on the solutions then the depth of the throat is naturally limited by the size of the flux quanta and, as in [23], we expect the red-shift of low-energy excitations near the bottom of the throat to yield an energy that matches the mass gap of the dual CFT.

We have also found that solutions that do not have a  $U(1) \times U(1)$  isometry can have a throat whose length depends both on the fluxes, and on geometric moduli of the base space. Most particularly, we have obtained *abyssal* solutions in which the depth of the throat can be made arbitrarily large by tuning certain angles on the base space! In these scaling solutions, the size of all the cycles remains finite as the length of the throat becomes larger and larger, and hence the solutions can be described using supergravity for arbitrarily lengths of the throat. While we have only constructed abyssal solutions corresponding to black rings, it is pretty clear that black hole microstates with this feature

could also be constructed this way. From a four-dimensional perspective, these solutions correspond to D6– $\overline{\text{D6}}$  solutions that have closed quivers, and hence the branes appear to get arbitrarily close to each other [40–43]. Nevertheless, that perspective is misleading: when considering the full five-dimensional solution, the physical distances between the GH points corresponding to the D6 branes remains *finite* throughout the scaling. Moreover, unlike their four-dimensional counterparts, the solutions that we consider are smooth.

The fact that one can construct smooth horizonless solutions that have arbitrarily long throats poses interesting questions for the interpretation of microstate geometries from the point of view of the *AdS/CFT* correspondence. Since these geometries are dual (up to  $1/N$  corrections) to states of the boundary CFT, it appears naively that these states will have an arbitrarily small mass-gap, as well as a whole tower of excitations that can be made arbitrarily light, contradicting expectations for a quantum theory in a box. Moreover, since the geometries we construct are supersymmetric and have very large cycles, and hence very low curvatures, one can imagine perturbing them slightly by adding a suitably small box of gas with some entropy, and doing this without significantly disturbing the geometries. If one then dials the length of the throat to become arbitrarily large one will obtain a system that has the entropy of the gas, but has an energy arbitrarily close to the BPS bound. In the following sub-sections we will refine these puzzles and discuss some possible resolutions.

### 6.1. *The spectrum and mass gaps in AdS/CFT: The puzzle*

The best-studied theory that is holographically dual to the geometries we consider is the D1-D5 CFT. At strong coupling this CFT is dual to string theory on  $AdS_3 \times S^3 \times T^4$ . Even though our geometries are constructed in eleven-dimensional supergravity, it is elementary to dualize them to the appropriate IIB frame. One then obtains a solution in which the D1 and D5 branes are wrapped on a common circle,  $C$ . To obtain a solution that is asymptotic to  $AdS_3 \times S^3 \times T^4$  one must also drop the constant terms in the harmonic functions associated with the D1-brane and D5-brane charges [46,36]. In doing this, the circle,  $C$ , decompactifies and becomes part of the  $AdS_3$  <sup>6</sup>.

It is often useful to consider the D1-D5 field theory in a finite-sized “box” and one of the simplest ways to do this is to restore the constants to the harmonic functions so that

---

<sup>6</sup> One should not confuse this  $AdS_3$  with that of the near-horizon limit of the supertube in M-theory: They are different, and the  $AdS_3$  of the IIB theory emerges non-trivially via the T-dualities.

the supergravity solution is asymptotically flat and the common circle,  $C$ , has a radius,  $R$ . At weak coupling, the perturbative string excitations must be quantized in mass units of  $\frac{1}{N_1 N_5 R}$  and so one expects the mass gap and the typical energy gap between states to be of this order. There are some issues as to whether this approach is well-defined in the strict sense of the  $AdS/CFT$  correspondence (see below); a more careful approach would be to introduce a UV cut-off in the radial direction of  $AdS_3$ . The effect of this is, once again, to introduce a scale in the bulk. More generally, anything that sets a finite scale for the spatial volume of the field theory direction at infinity also sets a mass scale for that theory.

Three-charge solutions that are asymptotically  $AdS_3 \times S^3 \times T^4$  also have additional, intermediate scales. For both black holes and black rings, there exists a scale  $r_p \sim \sqrt{Q_P}$  associated to the total momentum. This scale is set by the equal balance of the terms in the momentum harmonic function  $Z_P \approx 1 + Q_P/r^2$ . For black rings there are also scales set by the radius of the ring and by the dipole charges.

Since the  $AdS/CFT$  correspondence relates smooth, horizonless, asymptotically  $AdS$  solutions to states of the dual field theory, one can calculate, both in the bulk and on the boundary, the spectrum of non-BPS excitations above a given BPS state, and try to identify the boundary dual of a certain state by matching these spectra. These calculations have been very successful both for two-charge solutions [1,3], and for simple three-charge solutions [17]. This has allowed precise matching of bulk solutions with boundary states.

A rougher way to estimate the non-BPS mass gaps in the spectrum of excitations above a certain asymptotically-flat bulk solution is to consider the lowest energy oscillations localized in the throat of this solution. The corresponding mass gap, and indeed typical energy separation of states, in the holographic dual theory is then obtained by calculating the red-shifted energy of these excitations at infinity in the asymptotically flat solution<sup>7</sup>. For the D1-D5-P system, introducing a cut-off for evaluating the energy of excitations is not even necessary since the bulk solution already contains a scale associated to the momentum charge  $Q_P$ . The bulk energies redshifted to this scale correspond on the boundary to the ratio between the energy of the excitations and the energy coming from the total momentum.

---

<sup>7</sup> Alternatively, one can work entirely with an asymptotically  $AdS$  solution, that is cut off at a large, but finite distance,  $r = \frac{1}{\epsilon}$ , and impose appropriate boundary conditions on this surface [47]. The red-shifted bulk energy evaluated at the cutoff  $r = \frac{1}{\epsilon}$  can then be matched to the energy in the boundary theory placed in a box of size  $\frac{1}{\epsilon}$ .

For the deep microstate geometries, the non-BPS excitations about these states generically have a mass gap, and typical energy separation between states, that vary inversely with the depth of the throat in the bulk. For the  $U(1) \times U(1)$  invariant microstates, the spectrum coming from the deepest possible throats matches the lowest bound on the mass gap expected from the orbifold point description of the CFT, namely,  $E_0 = \frac{1}{N_1 N_5 R}$  [23]. Although we have not checked this explicitly, we also expect the mass gap of the deepest  $U(1) \times U(1)$  black ring microstates to match the mass gap expected from the orbifolded point description of black rings [46].

For microstates that do not have a  $U(1) \times U(1)$  invariance, we have the “abysses” in which the throat can become arbitrarily deep as a function of moduli. As the throat becomes deeper and deeper, all the excitations at the bottom of the throat become lighter and lighter, and the field theory spectrum approaches what looks like a continuum spectrum. Nevertheless, one does not expect this of a quantum theory that is confined in a box, however large. Since we are comparing spectra at different values of the coupling constants, and one might argue that strong coupling effects do not modify the spectrum of  $U(1) \times U(1)$  invariant configurations, but will modify the spectrum of the configurations with less symmetry, and allow states whose energy separations are much smaller than the expected weak-coupling value. However, for excitations above a given BPS state, these energy separations will not become arbitrarily small if the size of the box is kept fixed. Using condensed-matter language, when the mass of a very large number of excitations goes to zero one approaches a quantum critical point, and one does not expect to find quantum critical points in systems of finite size.

## 6.2. A possible resolution: Quantizing the moduli space

The simplest and most straightforward resolution of this abyssal conundrum would be to find a way of cutting off the throats of the scaling solutions at some finite value.

As we have already noted, the modulus in our example must be extremely finely tuned in order to obtain a very deep throat. In string theory, and even in supergravity, this moduli space will be quantized. Indeed, one can try to quantize it by considering the effective action for slow motions on the moduli space and then apply quantum mechanics (where Planck’s constant will be related to  $\frac{1}{N}$  effects). This will mean that there will be limits on our ability to precisely localize GH points on the GH base metric and thus localize the moduli sufficiently well to generate very deep throats. The effectiveness of this will depend on the details of the correct physical metric on the phase-space of the theory.



If the metric on the moduli space comes from the positions in the  $\mathbb{R}^3$  base of the GH geometry, then it may well provide an effective and useful cut-off. On the other hand, the phase space measure may well be related to the complete physical metric and it is hard to imagine how a quantization principle could cut-off a throat that is several megaparsecs long.

Putting this more graphically, suppose that one is given a smooth, horizonless, classical solution of arbitrarily low curvature and  $g_s$ , and that has a length  $10^{10}$  times larger than the maximum value consistent with mass gaps on the boundary theory, it is very hard to imagine that quantum effects, which are intrinsically of order  $1/N$ , will be able to destroy it. Note that the puzzle is *not* about destroying the very large throats by throwing particles from infinity. For an arbitrarily deep throat this can always be done, as any particle thrown in from infinity will eventually be blue-shifted enough going down the throat to destroy it. From the boundary perspective the very deep throats correspond to very finely tuned superpositions of eigenstates, and generic interactions with other states can easily destroy them. The fact that particles thrown in from infinity destroy the states does not make them physically irrelevant<sup>8</sup> (though it will probably imply that non-BPS microstates will not have arbitrarily long throats – see the discussion below). The puzzle comes from the *existence* and the physics of BPS microstates of arbitrary long throats, and the fact that the excitations that live at the bottom of the throat appear virtually massless from the point of view of the boundary theory.

Despite the concerns over “quantizing away” macroscopic geometries, there are natural ways in which this might be realized. For example, the angles on the base space could well be quantized because of the quantization of angular momentum. Given a certain bubbling solution, the value of  $J_R$  is determined entirely by the quantized fluxes on the bubbles (2.7), and hence it is automatically quantized. The angular momentum,  $J_L$ , defined in (2.8) and (2.9), not only depends upon the quantized flux but also upon the orientations of the bubbles. Continuously varying an angle will therefore generically yield non-integer values of  $J_L$ . While this is certainly true of the simple example considered in Section 5, and indeed will be true if one varies a single modulus in almost any solution, one can easily construct solutions in which there are moduli that do not change the total value of  $J_L$ . For example, one could make a scaling solution with two identical bubbling black rings on

---

<sup>8</sup> In the same way in which the fact that one can throw elephants and destroy a resonant cavity does not make the study of the modes of the cavity irrelevant.

opposite planes; alternatively one could consider a  $\mathbb{Z}_2$  symmetric bubbling black hole (like the “pincer” solution studied in [23]). These configurations, which have  $J_L = 0$  because of symmetry, can still become arbitrarily deep and it seems unlikely that any quantization coming from the *total* angular momentum could stop that.

On the other hand, one should also have some notion of a local quantization of the angular momentum. This is because, in some circumstances, it is possible to separate different components of a scaling solution in such a manner that it can be decomposed into separate classical objects; the  $J_L$  of each component must be quantized. It thus seems plausible that the individual contributions,  $\vec{J}_{L\,ij}$  in (2.11), coming from each bubble should be quantized. The *magnitude* of the  $\vec{J}_{L\,ij}$  is already quantized because of the quantization of fluxes, and so the non-trivial content of this statement lies in the quantization of the direction of  $\vec{J}_{L\,ij}$ . In such a picture, the total  $J_L$  in (2.12) would then be obtained by the standard rules for the addition of spins in quantum mechanics. If this picture were correct, then the ability to classically orient an individual bubble would be limited by the inverse of the magnitude of the flux that it carries. The fine tuning needed to create abysses would thus be limited. We are currently examining whether these angles are indeed quantized and how this limits the depth of throats.

Another possibility is that even if abysses exist, it does not make sense to talk about their mass gaps because even a very small particle at the bottom of a throat could have a large effect on the geometry and prevent the throat from becoming arbitrarily long. An example of this can occur in the “doubly-infinite”  $AdS_2$  throats that are encountered in the near-horizon geometry of black holes and black rings. As discussed in [48]<sup>9</sup>, such infinite throats can be destroyed by the energy-momentum tensor coming from a very small perturbation.

Since the throats of our solutions are capped, the metric near the cap is no longer of  $AdS \times S$  form. Therefore, extending the calculation of [48] to our solutions is not straightforward. If we naively assume equation (2.16) of [48] captures the essential physics, one can extend that analysis to our case. We find that a non-trivial energy-momentum tensor can be accommodated on top of our solutions provided the sphere shrinks to zero size at the cap. Fortunately, this is already happening even in the smooth BPS solutions, and is indeed a necessary feature of all the capped microstates. Hence, the obvious extension

---

<sup>9</sup> See equations (2.15) to (2.17) of that paper for more details.

of the argument in [48] does not rule out abyssal throats. It would be very interesting to see if one can construct an argument in a similar spirit that would cut off an abyss.

Summarizing this sub-section, it appears difficult to logically exclude the existence of some quantum mechanism that limits the depth of a throat. On the other hand, if this were to happen, this would be a rather remarkable first example of quantum effects destroying a very large portion of a smooth, horizonless, low-curvature, asymptotically-flat classical geometry.

### *6.3. A possible resolution: Stringent constraints on the duality*

Another possible resolution of the problem is to take the more “stringent” view that the  $AdS/CFT$  correspondence only relates field theories in an infinite volume to asymptotically  $AdS$  solutions without a cutoff. In this context calculations of mass gaps, times of flights, or energy spectra are, at best, of limited validity and, at worst, meaningless. From this perspective, the only thing one can meaningfully compute in the bulk are  $N$ -point functions. Indeed, by computing one-point functions in certain two-charge geometries and relating them to vev’s in the boundary theory it is possible to obtain a very precise mapping between bulk solutions and their dual boundary states [12], without appealing to spectra and mass-gaps.

This view poses the opposite problem: Why were mass-gap calculations in the D1-D5 system in a finite box so successful? One possible answer is that all these calculations were done for  $U(1) \times U(1)$  invariant microstates, and the extra symmetry “protects” the calculations done on the two sides of the duality, even if the duality is not strictly valid. Conversely, the microstates that do not have a  $U(1) \times U(1)$  invariance are not protected, and there is no reason why the calculations done in two inequivalent theories should agree. This answer is also consistent with the fact that mass-gaps computed in  $U(1) \times U(1)$  invariant three-charge microstates cannot be less than the smallest mass gap expected from the free (orbifold point) description of the CFT [23]. If this view is correct then one needs to understand what this protection mechanism is and why it works and why it fails.

There is also another rather puzzling feature of this perspective: While the D1-D5 system does not have a scale, the D1-D5-P system does have a scale set by  $Q_P$ . Even if it does not make sense to talk about the energy of excitations of arbitrarily deep throats by themselves, it does make sense to talk about the ratio between this excitation energy and the energy coming from the total momentum,  $Q_P$ . We therefore find that the energies of

excitations in an abyss are going to zero compared to the energy of the momentum excitations that are ultimately responsible for making the classical horizon area macroscopic. It would therefore seem that one could store very large amounts of entropy in such massless excitations.

## 7. Entropy elevators and non-BPS microstates.

We have thus two distinct, though logically possible outcomes, both of which are physically unexpected and both of which hint at tantalizing new phenomena. If abysses are cut off by quantum effects then these quantum effects can remove macroscopic portions of a low-curvature asymptotically-flat solution, and if the abysses are not cut off, then we appear to have a quantum critical point.

In trying to understand both of these possibilities we have found it useful to think about the effects of “entropy elevators.” The idea is to consider a small sub-system of non-BPS excitations and then adiabatically lower that sub-system into very deep throats so that the energy is red-shifted to the value determined by the depth of the throat and yet the entropy in the non-BPS excitations remains constant. There are two ways that one could imagine controlling such an elevator: Either by lowering the elevator using a massless cable or, as we prefer here, constructing the non-BPS excitations in a “shallow cap” and then adiabatically changing the modulus so that the cap descends to the bottom of a deep throat. If the moduli space is quantized then the elevator is only allowed to go to discrete floors and there is a lowest possible floor, but in an abyss there is no lower limit and all the excitations of that sub-system will become massless in the limit when the length of the throat approaches infinity. Hence, at the critical point the system has new massless modes.

For a given smooth cap there will be a limit on the size of the non-BPS sub-system: It must not significantly alter the physics of the cap and radically modify the elevator. In the limit when the throat is infinite, the extra mass will be zero and the state will, once again be (arbitrarily close to) BPS, and yet there will still be entropy in this sub-system. The solution will also be (arbitrarily close to) the classical BPS black hole. Hence, it is possible that one can only use microstate geometries to account for the entropy of the BPS black hole by considering all the throats that can act as “entropy elevators” that carry massive sub-systems of finite entropy to an infinite throat depth, where their mass becomes zero.

The entropy that a certain “elevator” can carry is limited by the requirement that the non-BPS sub-system added on does not destroy the solution. Note that this requirement has nothing to do with the energy seen from infinity, but rather with the effect of the sub-system on the bubbles that form the cap of the solution. Whether the sub-system destroys a certain cap, or not, has nothing to do with the length of the throat at whose end the cap is. The sub-system should only care about the local geometry of the cap and its presence should not limit the ability of the elevator to descend. The only effect of the throat is to make the energy of the sub-system as seen from infinity larger or smaller. Thus, for every cap we can associate a maximal “local” energy  $E_c$  that is the maximal energy that does not destroy it, and a certain entropy  $S_c$ . The mass above the BPS bound as seen from infinity is  $E_\infty = E_c \sqrt{g_{00}^{min}}$  where  $g_{00}^{min}$  is the value of  $g_{00}$  at the bottom of the throat. As the throat length approaches infinity, the elevator associated with each deep throat contributes with  $S_c$  to the entropy of the black hole. It is tempting to conjecture that the entropy of the BPS black holes comes entirely from these entropy elevators<sup>10</sup>.

The idea of lowering boxes containing entropy into black holes and studying the entropy in the process is not new in General Relativity and has led to apparent paradoxes and beautiful resolutions. See, for example, [49,50] and for recent work see also [51]. However, entropy elevators have two very different features. The first is that the box is lowered on top of a horizonless, BPS solution, and there is no Hawking radiation from the horizon to keep the box in equilibrium, or to allow the creation of box - anti-box pairs. The second is that the entropy in the elevators never goes into the entropy of a black hole: As the elevators descend, the solution always remains horizonless. Indeed, we will see below that as an elevator carrying a box of a certain “local” energy,  $E$ , descends, the energy as seen from infinity decreases, and the horizon of the corresponding black hole also descends at the same rate.

The idea of entropy elevators also has some interesting consequences for near-BPS black holes. These black holes have a finite throat depth, set by the non-extremality parameter. In the elevator picture, to create a finite amount of non-extremality one must add a finite amount of energy,  $\Delta E$ , above the BPS bound. To create this amount of energy at infinity by putting a non-BPS sub-system on an elevator means that the amount of energy on the elevator must be  $E_{local} = \Delta E / \sqrt{g_{00}}$ . At a certain depth this energy

---

<sup>10</sup> This would imply that the entropy of the D1-D5-P CFT at strong coupling has “accumulation points,” corresponding to the abysses.

will exceed the energy,  $E_c$ , needed to destroy the cap. Thus there is a limit to which the entropy elevator can descend for a given amount of non-extremality.

If the entropy elevators can be used to create near-BPS black hole microstates, the depth of the entropy elevators that carry most of the entropy should match the depth of the horizon of the near-BPS black hole. While a perfect matching of these two quantities is not possible without constructing the solutions corresponding to the elevators, one can check that the depth of the elevators and the “depth” of the horizon scale in the same way with the energy above extremality, which is a rather non-trivial check.

Indeed, given a certain energy,  $\Delta E$ , above the BPS bound, one can construct shallow entropy elevators, that have a sub-system of energy a few times  $\Delta E$ , as well as deeper elevators, that have a sub-system of energy  $E_{local} = \Delta E / \sqrt{g_{00}^{\text{bottom}}}$ . Clearly, the deeper elevators will carry a bigger system, and will have more entropy. If we make  $E_{local}$  bigger than the maximal energy a cap can support,  $E_c$ , then the elevator will be destroyed. Hence, most entropy will come from the elevators of depth corresponding to

$$g_{00}^{\text{bottom}} = (Z_1 Z_2 Z_3)^{-2/3} = \frac{(\Delta E)^2}{E_c^2}. \quad (7.1)$$

We can compare the depth of these elevators to the depth of the horizon of a near-BPS black hole. The easiest measure of the depth of that throat are the values of the three harmonic functions at the horizon, which in the near-BPS limit are given by:

$$Z_i \approx \frac{Q_i}{\Delta E} \quad (7.2)$$

Hence, the depth of the elevators and the depth of the near-BPS black hole horizon have the same dependence on  $\Delta E$ . This is a necessary feature if elevators are to give the microstates of the non-extremal black holes, and its confirmation is encouraging. It would be interesting to analyze in more detail the amount of energy,  $E_c$ , that a certain cap can carry, and see if its dependence on the charges also matches that predicted by equations (7.1) and (7.2).

Hence, if this idea of entropy elevators is correct, one should think about elevators that descend to an infinite depth as giving the entropy of the extremal black holes, and the elevators that descend to a finite depth as giving the entropy of the non-extremal black holes.

**Acknowledgments:** We would like to thank Davide Gaiotto, Eric Gimon, Juan Maldacena, Samir Mathur, Radu Roiban, Ashoke Sen, Kostas Skenderis, Marika Taylor and Xi Yin for interesting discussions. NPW would like to thank the SPhT, CEA-Saclay for hospitality while this work was completed. The work of NPW and CWW is supported in part by the DOE grant DE-FG03-84ER-40168. The work of IB was supported in part by the *Direction des Sciences de la Matière* of the *Commissariat à l'Énergie Atomique* of France and by the ANR grant BLAN06-3-137168.

## Appendix A. Verifying the absence of closed time-like curves

To check that there are no CTC's we must verify the standard set of conditions:

$$V Z_I \geq 0, \quad \mathcal{Q} \equiv Z_1 Z_2 Z_3 V - \mu^2 V^2 \geq 0. \quad (\text{A.1})$$

We have extensively examined these conditions numerically and found that they are satisfied for a broad sample of the scaling solutions given in Table 1. While the conditions, (A.1), are necessary, there is an additional dangerous term from the angular terms in the direction of the base metric:

$$(Z_1 Z_2 Z_3)^{1/3} V \left( dx^2 + dy^2 + dz^2 - \frac{\omega^2}{\mathcal{Q}} \right) \equiv (Z_1 Z_2 Z_3)^{1/3} V \bar{g}_{\mu\nu} dx^\mu dx^\nu. \quad (\text{A.2})$$

Since the positivity of the coefficient,  $(Z_1 Z_2 Z_3)^{1/3} V$ , has already been verified in checking (A.1), it remains to verify that  $\bar{g}_{\mu\nu}$  has no negative-norm vectors. The lowest eigenvalue of  $\bar{g}_{\mu\nu}$  must therefore be non-negative:

$$1 - \frac{|\omega|^2}{\mathcal{Q}} \geq 0. \quad (\text{A.3})$$

We checked this condition by cutting a slice near the ring and numerically evaluating this condition on this slice. We then moved this slice around to check the potentially dangerous region. In Figure 4, we show a particular slice that covers all three charges. We found that (A.3) was globally satisfied, and  $\mathcal{Q} - |\omega|^2$  was globally positive. Not only is this a more stringent condition than the last condition in (A.1), but, as was noted in [21], this means that the complete metric is stably causal and that the coordinate,  $t$ , provides a global time function.

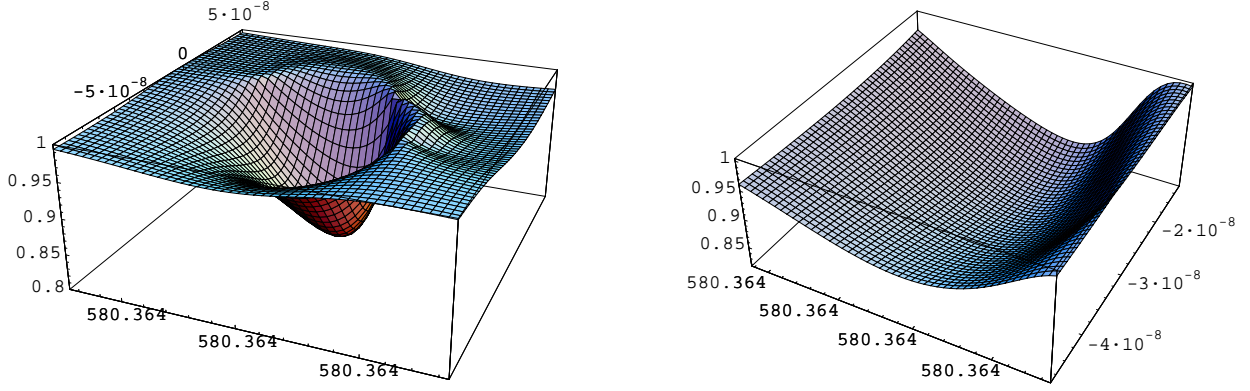


**Fig. 4:** These two graphs evaluate the condition (A.3) on the plane where all three charges are located for a particular triangle solution for which the three distances are  $\sim 10^{-8}$ . The first graph covers all three charges and the second graph shows a “zoom-in” at the bottom of the valley in the first graph.



## References

- [1] O. Lunin and S. D. Mathur, “AdS/CFT duality and the black hole information paradox,” Nucl. Phys. B **623**, 342 (2002) [arXiv:hep-th/0109154].
- [2] O. Lunin and S. D. Mathur, “Statistical interpretation of Bekenstein entropy for systems with a stretched horizon,” Phys. Rev. Lett. **88**, 211303 (2002) [arXiv:hep-th/0202072].
- [3] O. Lunin, J. M. Maldacena and L. Maoz, “Gravity solutions for the D1-D5 system with angular momentum,” arXiv:hep-th/0212210.
- [4] O. Lunin and S. D. Mathur, “The slowly rotating near extremal D1-D5 system as a ‘hot tube’,” Nucl. Phys. B **615**, 285 (2001) [arXiv:hep-th/0107113].
- [5] L. F. Alday, J. de Boer and I. Messamah, “The gravitational description of coarse grained microstates,” JHEP **0612**, 063 (2006) [arXiv:hep-th/0607222].
- [6] A. Donos and A. Jevicki, “Dynamics of chiral primaries in  $AdS(3) \times S^3 \times T^4$ ,” Phys. Rev. D **73**, 085010 (2006) [arXiv:hep-th/0512017].
- [7] L. F. Alday, J. de Boer and I. Messamah, “What is the dual of a dipole?,” Nucl. Phys. B **746**, 29 (2006) [arXiv:hep-th/0511246].
- [8] S. Giusto, S. D. Mathur and Y. K. Srivastava, “Dynamics of supertubes,” Nucl. Phys. B **754**, 233 (2006) [arXiv:hep-th/0510235].
- [9] M. Taylor, “General 2 charge geometries,” JHEP **0603**, 009 (2006) [arXiv:hep-th/0507223].
- [10] K. Skenderis and M. Taylor, “Fuzzball solutions and D1-D5 microstates,” Phys. Rev. Lett. **98**, 071601 (2007) [arXiv:hep-th/0609154].
- [11] I. Kanitscheider, K. Skenderis and M. Taylor, “Holographic anatomy of fuzzballs,” JHEP **0704**, 023 (2007) [arXiv:hep-th/0611171].
- [12] I. Kanitscheider, K. Skenderis and M. Taylor, “Fuzzballs with internal excitations,” arXiv:0704.0690 [hep-th].
- [13] S. D. Mathur, “The quantum structure of black holes,” Class. Quant. Grav. **23**, R115 (2006) [arXiv:hep-th/0510180]. S. D. Mathur, “The fuzzball proposal for black holes: An elementary review,” Fortsch. Phys. **53**, 793 (2005) [arXiv:hep-th/0502050].
- [14] I. Bena and P. Kraus, “Three charge supertubes and black hole hair,” Phys. Rev. D **70**, 046003 (2004) [arXiv:hep-th/0402144].
- [15] S. Giusto, S. D. Mathur and A. Saxena, “Dual geometries for a set of 3-charge microstates,” Nucl. Phys. B **701**, 357 (2004) [arXiv:hep-th/0405017].
- [16] O. Lunin, “Adding momentum to D1-D5 system,” JHEP **0404**, 054 (2004) [arXiv:hep-th/0404006].
- [17] S. Giusto, S. D. Mathur and A. Saxena, “3-charge geometries and their CFT duals,” Nucl. Phys. B **710**, 425 (2005) [arXiv:hep-th/0406103].

- [18] S. D. Mathur, A. Saxena and Y. K. Srivastava, “Constructing ‘hair’ for the three charge hole,” Nucl. Phys. B **680**, 415 (2004) [arXiv:hep-th/0311092].
- [19] S. Giusto and S. D. Mathur, “Geometry of D1-D5-P bound states,” Nucl. Phys. B **729**, 203 (2005) [arXiv:hep-th/0409067].
- [20] I. Bena and N. P. Warner, “Bubbling supertubes and foaming black holes,” Phys. Rev. D **74**, 066001 (2006) [arXiv:hep-th/0505166].
- [21] P. Berglund, E. G. Gimon and T. S. Levi, “Supergravity microstates for BPS black holes and black rings,” JHEP **0606**, 007 (2006) [arXiv:hep-th/0505167].
- [22] I. Bena, C. W. Wang and N. P. Warner, “The foaming three-charge black hole,” arXiv:hep-th/0604110.
- [23] I. Bena, C. W. Wang and N. P. Warner, “Mergers and typical black hole microstates,” JHEP **0611**, 042 (2006) [arXiv:hep-th/0608217].
- [24] J. Ford, S. Giusto and A. Saxena, “A class of BPS time-dependent 3-charge microstates from spectral flow,” arXiv:hep-th/0612227.
- [25] M. C. N. Cheng, “More bubbling solutions,” JHEP **0703**, 070 (2007) [arXiv:hep-th/0611156].
- [26] I. Bena and N. P. Warner, “Black holes, black rings and their microstates,” arXiv:hep-th/0701216.
- [27] I. Bena and P. Kraus, “Microstates of the D1-D5-KK system,” Phys. Rev. D **72**, 025007 (2005) [arXiv:hep-th/0503053].
- [28] A. Saxena, G. Potvin, S. Giusto and A. W. Peet, “Smooth geometries with four charges in four dimensions,” JHEP **0604**, 010 (2006) [arXiv:hep-th/0509214].
- [29] V. Balasubramanian, E. G. Gimon and T. S. Levi, “Four Dimensional Black Hole Microstates: From D-branes to Spacetime Foam,” arXiv:hep-th/0606118.
- [30] Y. K. Srivastava, “Perturbations of supertube in KK monopole background,” arXiv:hep-th/0611320.
- [31] F. Denef, D. Gaiotto, A. Strominger, D. Van den Bleeken and X. Yin, “Black hole deconstruction,” arXiv:hep-th/0703252.
- [32] V. Jejjala, O. Madden, S. F. Ross and G. Titchener, “Non-supersymmetric smooth geometries and D1-D5-P bound states,” Phys. Rev. D **71**, 124030 (2005) [arXiv:hep-th/0504181].
- [33] E. G. Gimon, T. S. Levi and S. F. Ross, “Geometry of non-supersymmetric three-charge bound states,” arXiv:0705.1238 [hep-th].
- [34] I. Bena, C. W. Wang and N. P. Warner, “Sliding rings and spinning holes,” JHEP **0605**, 075 (2006) [arXiv:hep-th/0512157].
- [35] I. Bena and N. P. Warner, “One ring to rule them all ... and in the darkness bind them?,” Adv. Theor. Math. Phys. **9**, 667 (2005) [arXiv:hep-th/0408106].
- [36] H. Elvang, R. Emparan, D. Mateos and H. S. Reall, “Supersymmetric black rings and three-charge supertubes,” Phys. Rev. D **71**, 024033 (2005) [arXiv:hep-th/0408120].

- [37] J. P. Gauntlett and J. B. Gutowski, “General concentric black rings,” *Phys. Rev. D* **71**, 045002 (2005) [arXiv:hep-th/0408122].
- [38] I. Bena, “Splitting hairs of the three charge black hole,” *Phys. Rev. D* **70**, 105018 (2004) [arXiv:hep-th/0404073].
- [39] H. Elvang, R. Emparan, D. Mateos and H. S. Reall, “A supersymmetric black ring,” *Phys. Rev. Lett.* **93**, 211302 (2004) [arXiv:hep-th/0407065].
- [40] F. Denef, “Supergravity flows and D-brane stability,” *JHEP* **0008**, 050 (2000) [arXiv:hep-th/0005049].
- [41] F. Denef, “Quantum quivers and Hall/hole halos,” *JHEP* **0210**, 023 (2002) [arXiv:hep-th/0206072].
- [42] B. Bates and F. Denef, “Exact solutions for supersymmetric stationary black hole composites,” arXiv:hep-th/0304094.
- [43] F. Denef and G. W. Moore, “Split states, entropy enigmas, holes and halos,” arXiv:hep-th/0702146.
- [44] E. G. Gimon and T. S. Levi, “Black Ring Deconstruction,” arXiv:0706.3394 [hep-th].
- [45] J. P. Gauntlett and J. B. Gutowski, “Concentric black rings,” *Phys. Rev. D* **71**, 025013 (2005) [arXiv:hep-th/0408010].
- [46] I. Bena and P. Kraus, “Microscopic description of black rings in AdS/CFT,” *JHEP* **0412**, 070 (2004) [arXiv:hep-th/0408186].
- [47] D. Z. Freedman, S. D. Mathur, A. Matusis and L. Rastelli, “Correlation functions in the CFT( $d$ )/AdS( $d + 1$ ) correspondence,” *Nucl. Phys. B* **546**, 96 (1999) [arXiv:hep-th/9804058].
- [48] J. M. Maldacena, J. Michelson and A. Strominger, “Anti-de Sitter fragmentation,” *JHEP* **9902**, 011 (1999) [arXiv:hep-th/9812073].
- [49] W. G. Unruh and R. M. Wald, ‘Acceleration Radiation And Generalized Second Law Of Thermodynamics,’ *Phys. Rev. D* **25**, 942 (1982).
- [50] W. G. Unruh and R. M. Wald, “Entropy Bounds, Acceleration Radiation, And The Generalized Second Law,” *Phys. Rev. D* **27**, 2271 (1983).
- [51] D. Marolf and R. Sorkin, “Perfect mirrors and the self-accelerating box paradox,” *Phys. Rev. D* **66**, 104004 (2002) [arXiv:hep-th/0201255].